Supporting Information

Efficient N_2 electroreduction to ammonia in isopropanol-PBS electrolyte by $NiFe_2O_4$ in situ grown on nickel foam

Chang Chen,‡[a,b] Min Cui,‡[a] Qian Wang,*[b] Penglei Cui,[b] Cong Zhang,[a] Qian Yang,[b] Jujie Ren*[a]

[a]Hebei Provincial Key Laboratory of Photoelectric Control on Surface and Interface, School of Sciences, Hebei University of Science and Technology, Shijiazhuang 050018, P.R. China.

[b]CAS Key Laboratory of Green Process and Engineering, State Key Laboratory of Multiphase Complex Systems, Beijing Key Laboratory of Ionic Liquids Clean Process, Institute of Process Engineering, Chinese Academy of Science, Beijing 100190, P.R. China.

Corresponding Authors
Email: wangq@ipe.ac.cn, jujieren@163.com

Ammonia detection

The yield of NH_3 in electrocatalytic nitrogen reduction was determined by indophenol blue method.

Regents used:

1) Coloring solution: 0.05 mol L^{-1} sodium hypochlorite solution.
2) Oxidation solution: 5% salicylic acid solution (Dissolve 10 g of salicylic acid, 10 g of Sodium citrate and 0.8 g of sodium hydroxide in 200 ml of deionized water.)
3) Catalyst solution: 1.0g $Na_2[Fe(CN)_5NO] \bullet 2H_2O$ diluted to 10ml with deionized water.
4) Absorption solution: 0.1M H_2SO_4 solution.
5) Standard ammonium solution: 0.3142g NH_4Cl after drying at 105℃ for 1h, it is dissolved in 100ml absorption solution to obtain an ammonia content of 1.00mg mL^{-1}, dilute to 1.00μgmL^{-1} with absorption solution before use.

Procedure:

2 mL of sample was taken. Then 0.2 mL of catalyst solution, 2 mL oxidation solution and 1 mL of coloring solution were added respectively to the sample solution. Absorbance measurements were performed after 1 h at λ=655 nm.

Determination of FE and NH_3 yield:

The FE for N_2 reduction was defined as the amount of electric charge used for synthesizing NH_3 divided the total charge passed through the electrodes during the electrolysis. Assuming three electrons were needed to produce one NH_3 molecule, the NH_3 yield could be calculated as follows:

$$NH_3 \ \ yield = \frac{[NH_3]V}{At} \qquad (1)$$

FE was calculated using the following equation:

$$FE = \frac{3F[NH_3]V}{17Q}\ 100\% \qquad (2)$$

Where:

F is the Faraday constant;

$[NH_3]$ is the measured NH_3 concentration;

V is the volume of the electrolyte in the cathodic chamber;

Q is the total quantity of applied electricity;

t is the reduction time;

A is the geometric area of the electrode.

Hydrazine detection

The Possible products of N_2H_4 in electrocatalytic nitrogen reduction were determined by Watt and Chrisp methods.

Regents used:

1) Coloring solution: Dissolve 1.2g $(CH_3)_2NC_6H_4CHO$ in 6 ml HCl and 60 ml Ethanol.
2) Standard hydrazine solution: 60.1 μL hydrazine solution, dilute to 25ml with a solution composed of the same electrolyte, and the hydrazine concentration is 2 mg mL^{-1}. Take 20 μL of the above solution and dilute it again to 20 ml, and the final hydrazine concentration is 2 μg mL^{-1}.

Procedure:

Prepare hydrazine standard solutions of different concentrations, dilute them to 5 ml with electrolyte, and add to 5 ml coloring solution. Absorbance measurements were performed after 30 min at λ=658 nm, The standard curve equation is obtained according to the relationship between absorbance and concentration. Take 5 ml of electrolytic solution and add 5 ml of developer to measure its absorbance.

Nitrogen solubility test

The fully automatic gas solubility detector is used to test the solubility of nitrogen in different systems, this instrument is based on the tube in tube micro membrane reactor, which can realize gas-liquid equilibrium in 10~30s, and realize rapid determination of gas-liquid properties through online flow.

Measuring principle:

The solubility C_i of gas in liquid can be expressed by Henry formula:

$$C_i = K_H P_i \qquad (3)$$

In the reactor, the gas transmembrane flux F_G is equal to the amount of gas dissolved in liquid:

$$C_i = \frac{F_G}{F_L V_s} \qquad (4)$$

When balancing, the balanced partial pressure P_i Equal to the total gas pressure P_G and the equilibrium pressure of the substance in the liquid phase in the gas phase P_i^V:

$$P_i = P_G - P_i^V \qquad (5)$$

The above equations are combined:

$$K_H = \frac{F_G}{F_L V_S (P_G P_i^V)} P_G - P_i^V \qquad (6)$$

Therefore, by using the Ramping method, the program controls the liquid flow to change continuously at a certain rate, while recording the corresponding gas flow change, fitting the experimental data to obtain the slope of F_G-F_L, and then the Henry coefficient can be measured.

Fig. S1. Experimental apparatus of the electrochemical reduction of N_2 to NH_3.

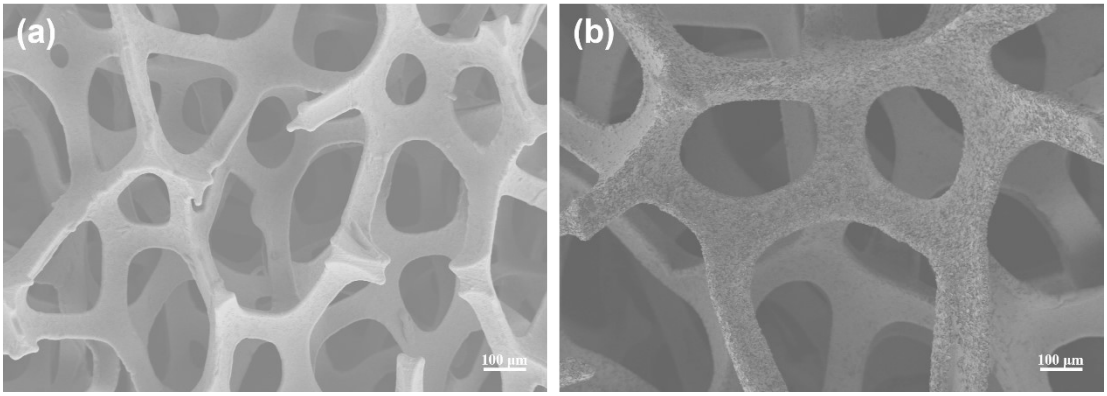

Fig. S2. SEM image of (a) bare NF and (b) $NiFe_2O_4$/NF.

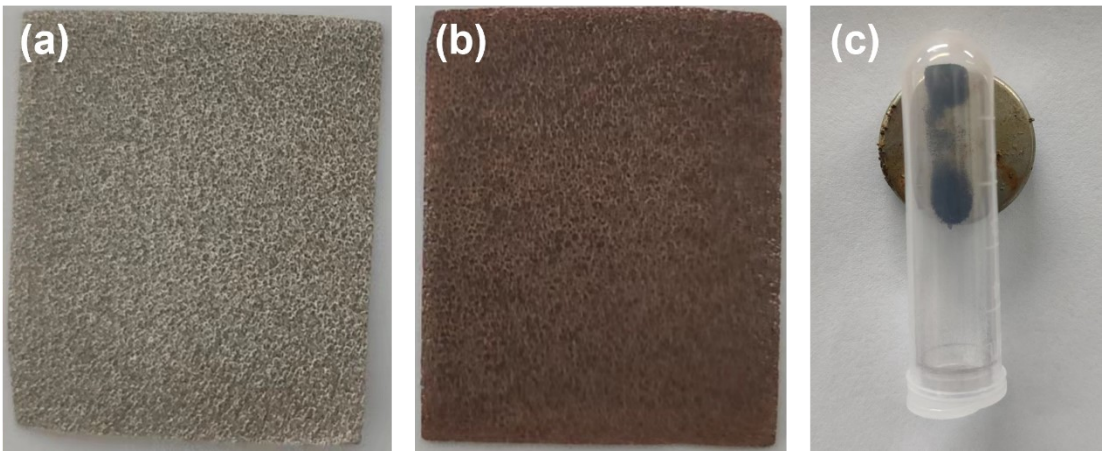

Fig. S3. Optical image of (a) bare NF, (b) $NiFe_2O_4$/NF and (c) magnetic absorption experiment.

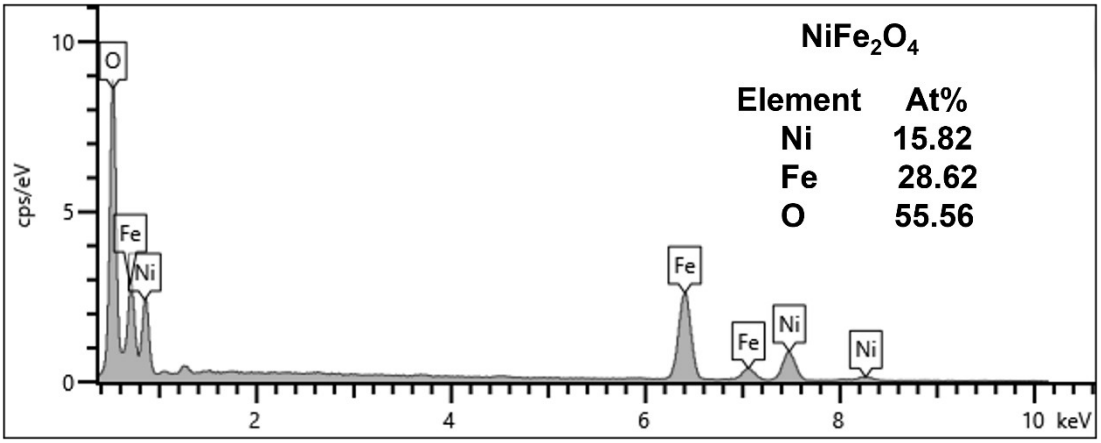

Fig. S4. EDS spectra of $NiFe_2O_4$ scraped off $NiFe_2O_4$/NF.

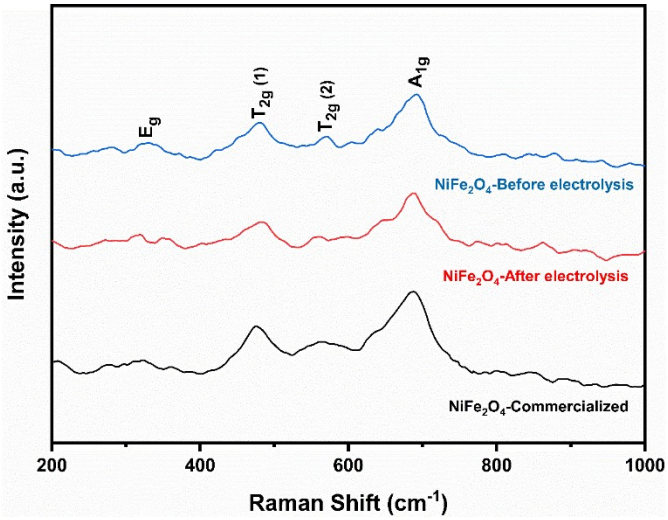

Fig. S5. Raman spectra of $NiFe_2O_4$.

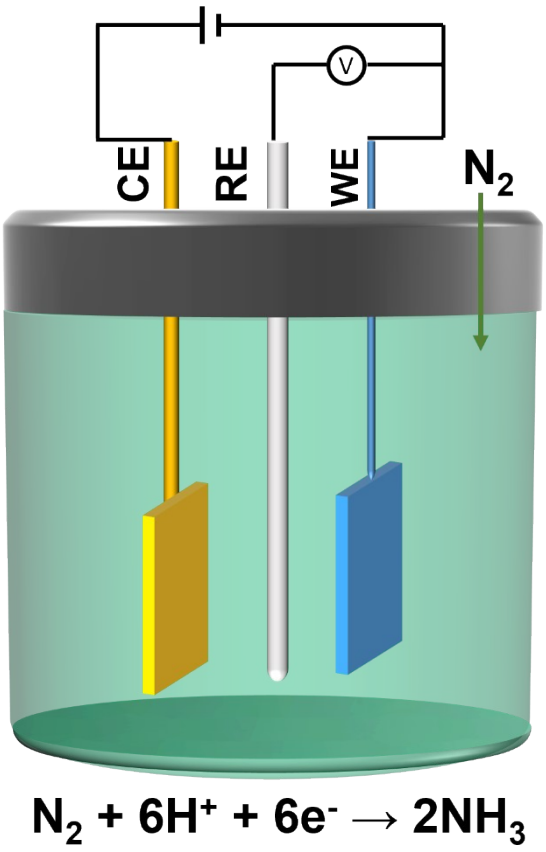

Fig. S6. Schematic diagram of ENRR process.

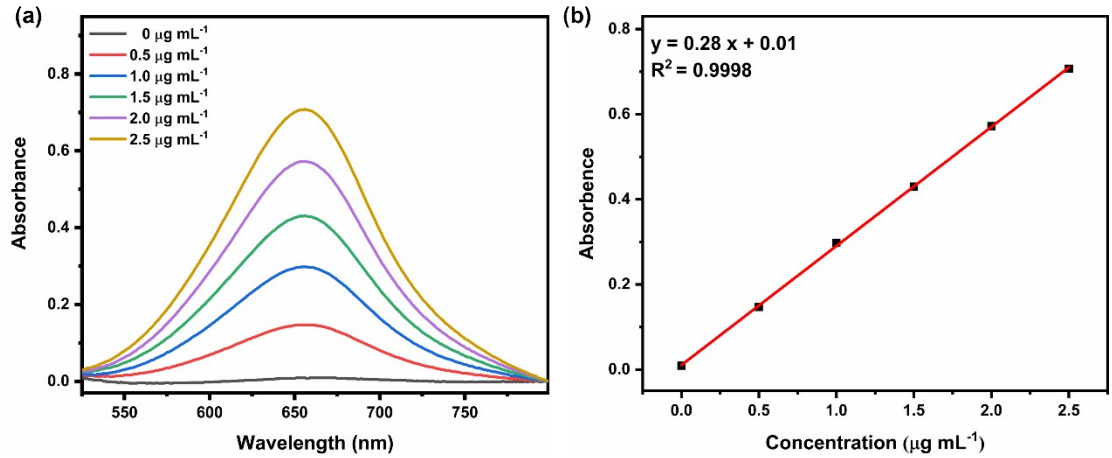

Fig. S7. (a) UV-Vis curves of indophenol assays with NH_4^+ ions after incubated for 60 mins (2-propanol+PBS). (b) Calibration curve used for estimation of NH_3 by NH_4^+ ion of different concentrations.

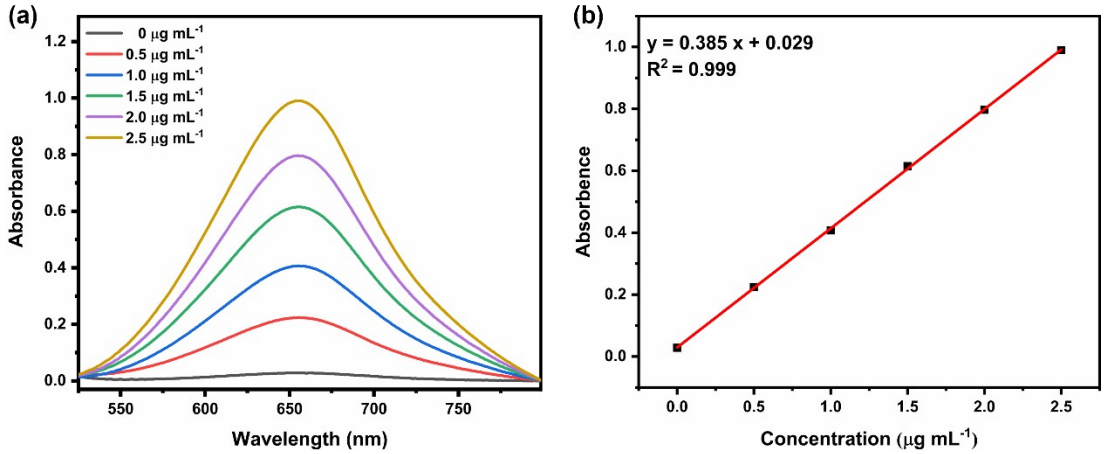

Fig. S8. (a) UV-Vis curves of indophenol assays with NH_4^+ ions after incubated for 60 mins (0.1mol L^{-1} H_2SO_4). (b) Calibration curve used for estimation of NH_3 by NH_4^+ ion of different concentrations.

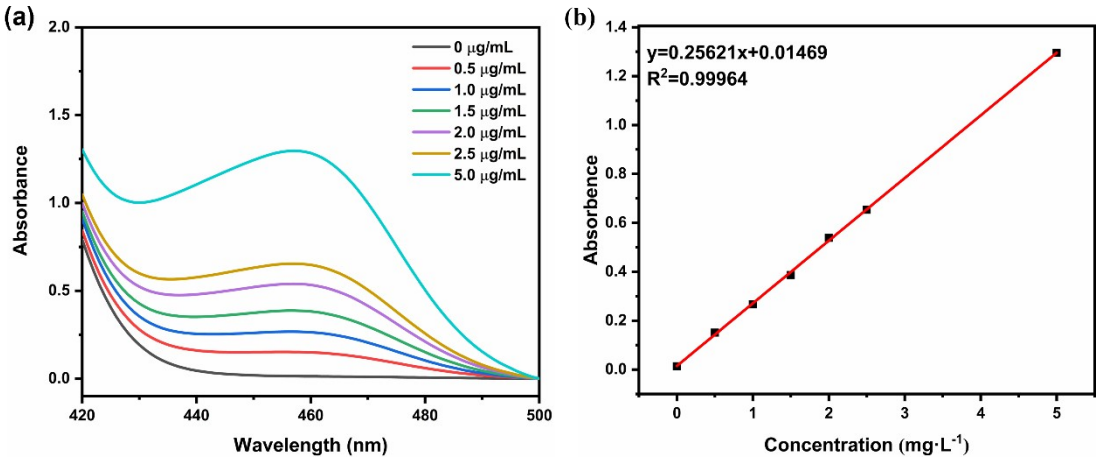

Fig. S9. (a) UV-Vis absorption spectra of various N_2H_4 concentration after incubated for 20 min at room temperature. (b) Calibration curve used for calculation of N_2H_4 concentration.

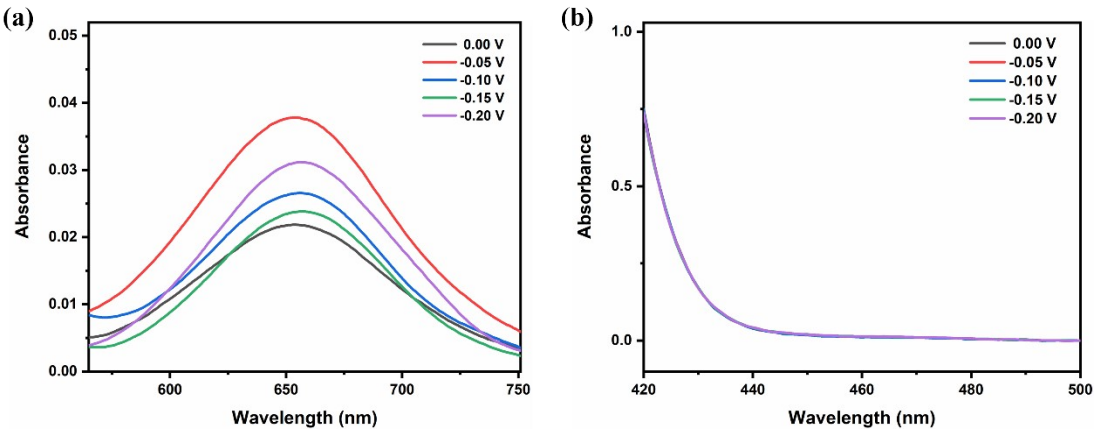

Fig. S10. UV–Vis absorption spectra of (a) the electrolytes stained with indophenol indicator during the 2 h electrolysis process on $NiFe_2O_4$/NF under different potentials, and (b) the electrolytes estimated by the method of Watt and Chrisp indicator during the 2 h electrolysis process on $NiFe_2O_4$/NF under different potentials.

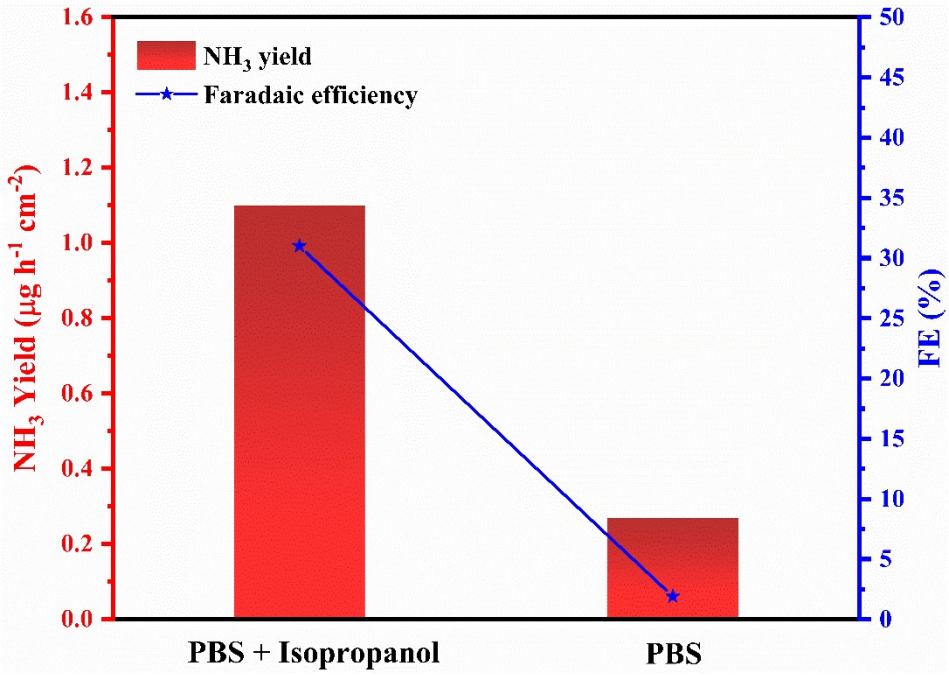

Fig. S11. Comparison of NH_3 yield and faradaic efficiency of different electrolytes.

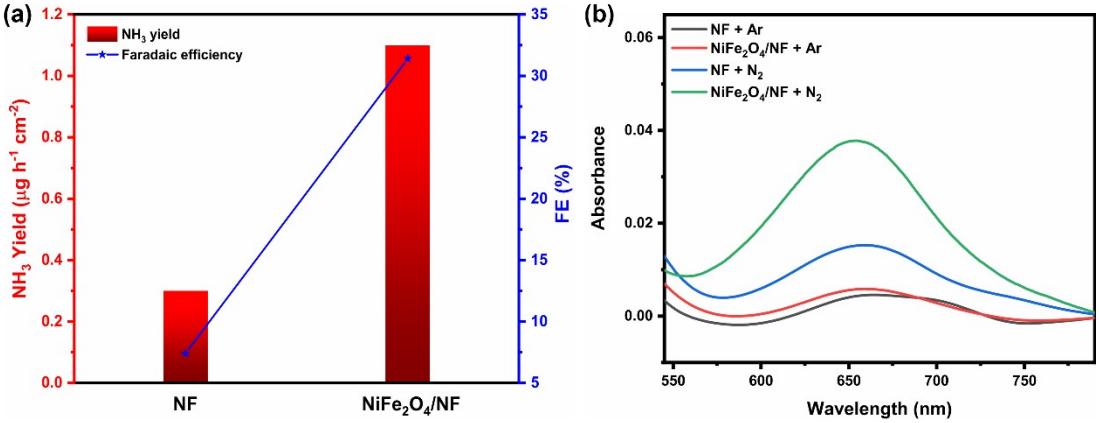

Fig. S12. (a) NH_3 yield rates and Faradaic efficiencies of bare NF and $NiFe_2O_4$/NF at -0.05V. (b) The control test was conducted to eliminate the NH_3 pollution caused by the environment.

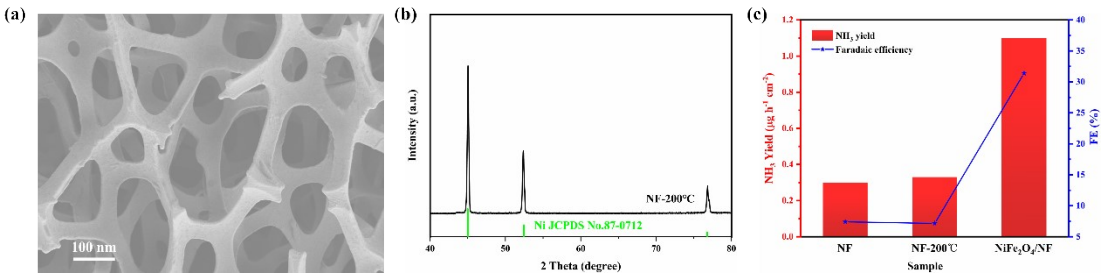

Fig. S13. (a) SEM image of NF-200℃. (b) XRD patterns of NF-200℃. (c) Comparison of NH_3 yield and FE of the three electrodes at -0.05V vs RHE.

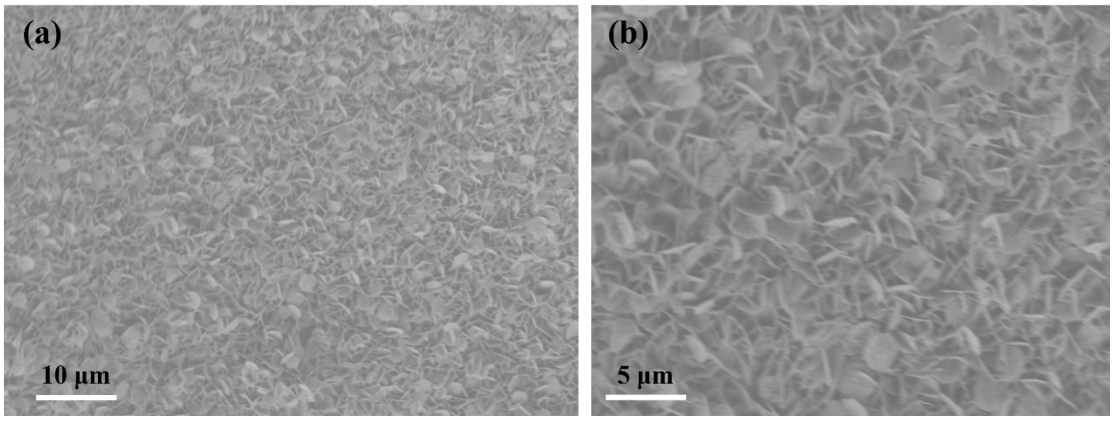

Fig. S14. SEM image of $NiFe_2O_4$/NF-After Electrolysis 10h.

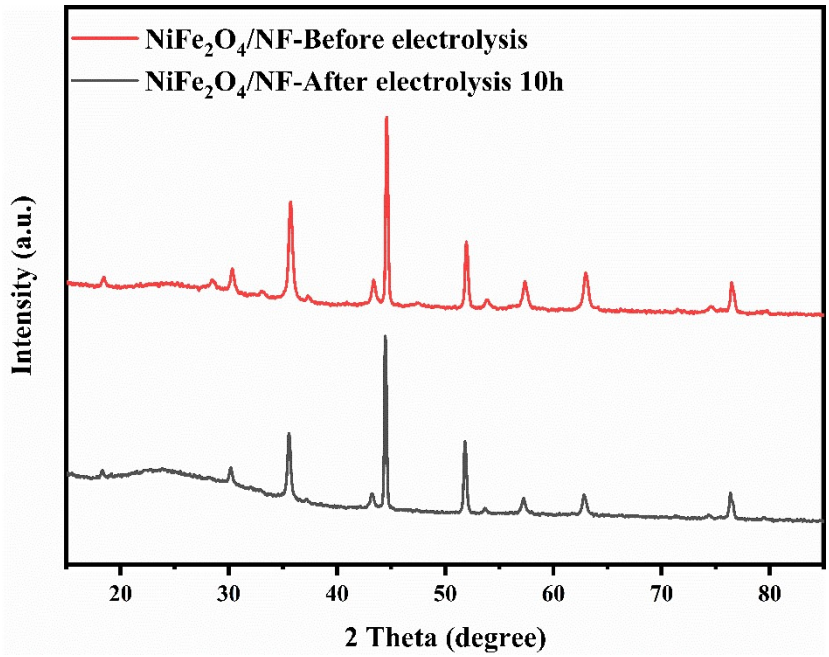

Fig. S15. XRD patterns of $NiFe_2O_4$/NF-Before electrolysis and $NiFe_2O_4$/NF-After electrolysis 10h.

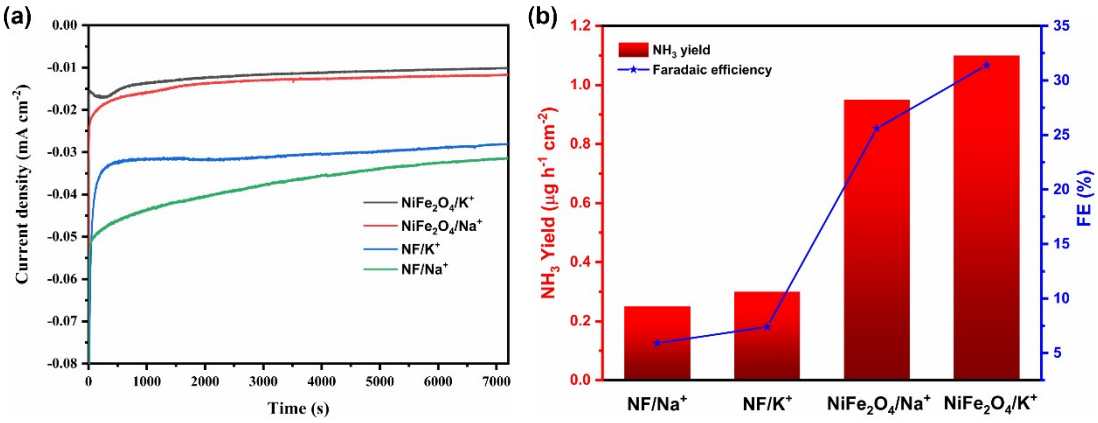

Fig. S16. Comparison of two electrodes of ENRR in 0.1mol L^{-1} PBS electrolyte composed of different ions. (a) i-t curves for the N_2RR on the two electrodes at E=-0.05 V (vs RHE). (b) NH_3 yield rates and Faradaic efficiencies of two electrodes at -0.05 V.

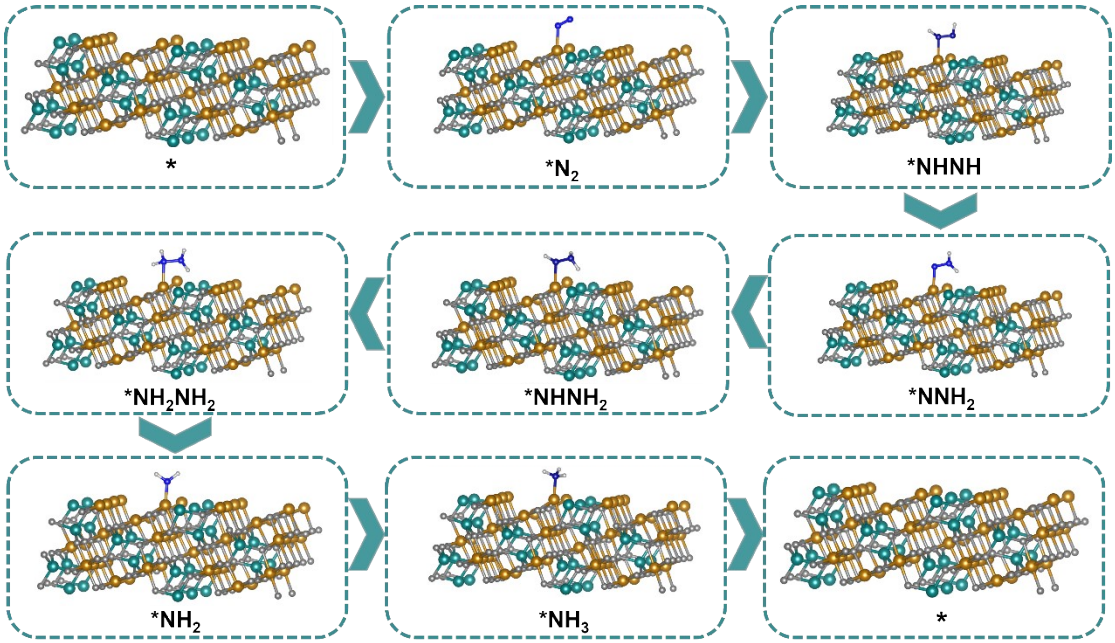

Fig. S17. Schematic diagram of atomic structure of alternative hydrogenation ENRR mechanism (Blue, brown, cyan, white and gray balls represent N, Fe, Ni, H and O, respectively).

Table S1. Comparison of the electrocatalytic activity of $NiFe_2O_4$/NF to produce NH_3 through ENRR with respect to the performances of other previously reported Ni, Fe based electrocatalysts.

Cathode	Electrolyte	Anode	Potential (vs. RHE)	NH_3 yield ($\mu g\ h^{-1}\ cm^{-2}$)	FE (%)	Ref.
Fe_3O_4/Ti	0.1M Na_2SO_4	Graphite	-0.4 V	3.43	2.6	[1]
Porous Ni	H_2SO_4/2-Propanol	Pt	3.5 V bias	1.07	0.9	[2]
Fe/CNT	Nafion/GDL	Pt	-0.2 V	0.22	0.03	[3]
Fe/Fe_3O_4	0.1M PBS	Pt	-0.3 V	0.19	8.29	[4]
$CoFe_2O_4$/rGO	0.1M Na_2SO_4	Pt	-0.4 V	2.57	6.2	[5]
Zr/α -FeOOH	0.1M Na_2SO_4	Pt	-0.5 V	8.5	35.63	[6]
Fe /FTO	$[P_{6,6,6,14}]$ [eFAP]	Pt	-0.8 V	0.29	60	[7]
$NiFe_2O_4$/NF	**2-Propanol/PBS**	**Pt**	**-0.65 V vs SCE**	**1.1**	**31.4**	**This work**

1 Q. Liu, X. Zhang, B. Zhang, Y. Luo, G. Cui, F. Xie and X. Sun, *Nanoscale*, 2018, **10**, 14386–14389.

2 K. Kim, N. Lee, C.-Y. Yoo, J.-N. Kim, H. C. Yoon and J.-I. Han, *J. Electrochem. Soc.*, 2016, **163**, F610–F612.

3 S. Chen, S. Perathoner, C. Ampelli, C. Mebrahtu, D. Su and G. Centi, *Angew. Chemie - Int. Ed.*, 2017, **56**, 2699–2703.

4 L. Hu, A. Khaniya, J. Wang, G. Chen, W. E. Kaden and X. Feng, *ACS Catal.*, 2018, **8**, 9312–9319.

5 M. I. Ahmed, S. Chen, W. Ren, X. Chen and C. Zhao, *Chem. Commun.*, 2019, **55**, 12184–12187.

6 J. Tan, X. He, F. Yin, X. Liang, G. Li and Z. Li, *Appl. Surf. Sci.*, 2021, **567**, 150801.

7 M. Ali, F. Zhou, K. Chen, C. Kotzur, C. Xiao, L. Bourgeois, X. Zhang and D. R. MacFarlane, *Nat. Commun.*, 2016, **7**, 1–5.